Available online at www.sciencedirect.com

ScienceDirect

Biochimica et Biophysica Acta 1778 (2008) 206–213

Biochimica et Biophysica Acta BBA

www.elsevier.com/locate/bbamem

Relevance of the N-terminal NLS-like sequence of the prion protein for membrane perturbation effects

Kamila Oglęcka [a], Pontus Lundberg [b], Mazin Magzoub [a,1], L.E. Göran Eriksson [a], Ülo Langel [b], Astrid Gräslund [a,*]

[a] *Department of Biochemistry and Biophysics, The Arrhenius Laboratories, Stockholm University, S-106 91 Stockholm, Sweden*
[b] *Department of Neurochemistry and Neurotoxicology, Stockholm University, S-106 91 Stockholm, Sweden*

Received 23 June 2007; received in revised form 28 August 2007; accepted 23 September 2007
Available online 10 October 2007

Abstract

We investigated the nuclear localization-like sequence KKRPKP, corresponding to the residues 23–28 in the mouse prion protein (mPrP), for its membrane perturbation activity, by comparing effects of two mPrP-derived peptides, corresponding to residues 1–28 (mPrPp(1–28)) and 23–50 (mPrPp(23–50)), respectively. In erythrocytes, mPrPp(1–28) induced ~60% haemoglobin leakage after 30 min, whereas mPrPp(23–50) had negligible effects. In calcein-entrapping, large unilamellar vesicles (LUVs), similar results were obtained. Cytotoxicity estimated by lactate dehydrogenase leakage from HeLa cells, was found to be ~12% for 50 μM mPrPp(1–28), and ~1% for 50 μM mPrPp(23–50). Circular dichroism spectra showed structure induction of mPrPp(1–28) in the presence of POPC:POPG (4:1) and POPC LUVs, while mPrPp(23–50) remained a random coil. Membrane translocation studies on live HeLa cells showed mPrPp(1–28) co-localizing with dextran, suggesting fluid-phase endocytosis, whereas mPrPp(23–50) hardly translocated at all. We conclude that the KKRPKP-sequence is not sufficient to cause membrane perturbation or translocation but needs a hydrophobic counterpart.

Keywords: Prion protein; Membrane translocation; Calcein leakage; Endosomal escape; NLS-like sequence; Haemoglobin leakage

1. Introduction

Transmissible spongiform encephalopathies (TSEs), also known as prion diseases, are fatal neurological disorders of humans and animals that can occur sporadically, by infection, or can be hereditary. The disorders are thought to be caused by a conversion of the cellular form of the neural prion protein (PrP^C), into an infectious scrapie isoform (PrP^{Sc}) [1–3]. The conversion is posttranslational and mutations of the primary amino acid sequence are not needed for the conversion to take place. PrP^{Sc} forms insoluble aggregates that show high resistance to proteinase K digestion, whereas PrP^C is monomeric and is readily digested via proteolytic processes [4].

The prion protein consists of an unstructured N-terminal domain (composed of a signal peptide (1–22) in the mouse protein), a basic region (23–28), a preoctarepeat region (29–50), an octarepeat region (51–105) prone to bind copper-ions, and a hydrophobic stretch (106–125), a globular C-terminal domain (126–231) comprised of three α-helices and two β-turns, and a C-terminal signal peptide (232–254) [5].

The full length prion protein is rarely examined together with its signal peptide (residues 1–22) since the signal peptide part is normally cleaved off during maturation. It has however been shown that in some cases this part can be retained [6], and that this particular sequence might be associated with functions such

Abbreviations: NLS, Nuclear Localization Sequence; PrP, Prion Protein; PrP^C, cellular isoform of PrP; PrP^{Sc}, scrapie isoform of PrP; mPrPp(1–28), residues 1–28 of the mouse PrP sequence; mPrPp(23–50), residues 23–50 of the mouse PrP sequence; bPrPp(1–30), residues 1–30 of the bovine PrP sequence; CD, Circular Dichroism; LUVs, Large Unilamellar Vesicles; hRBC, Human Red Blood Cell; POPC, 1-palmitoyl-2-oleoyl-*sn*-glycero-3-phosphocholine; POPG, 1-palmitoyl-2-oleoyl-*sn*-glycero-3-[phospho-*rac*-(1-glycerol)] sodium salt; LDH, Lactate Dehydrogenase; CPP, Cell-Penetrating Peptide; PTD, Protein Transduction Domain; HeLa cells, Henrietta Lacks cells; CHO cells, Chinese Hamster Ovary cells; TSE, Transmissible Spongiform Encephalopathies

* Corresponding author. Tel.: +46 8 162450; fax: +46 8 155597.
E-mail address: astrid@dbb.su.se (A. Gräslund).
[1] Present address: Department of Medicine and Physiology, University of California, San Francisco, CA 94143-0521, USA.

0005-2736/$ - see front matter © 2007 Elsevier B.V. All rights reserved.
doi:10.1016/j.bbamem.2007.09.034

as targeting and topogenesis [6–8]. It has also been proposed that the uncleaved signal peptide could cause the prion protein to change its conformation and thus become neurotoxic [6,9]. Hypothetically the mature PrP^C might even play a neuroprotective role, reversing neurotoxicity induced by the doppel (Dpl) protein, which is a PrP homologue. Deletion of the charged region PrPΔ(23–28) left the mutated PrP incapable of rescuing cerebellar neurons in transgenic mice [5].

The signal peptide is by itself hydrophobic and relatively insoluble in water, but taken together with the highly positive, nuclear localization-like (NLS-like) [10] KKRPKP-sequence (residues 23–28), it becomes water soluble. The corresponding peptide has a sequence that resembles the composition of certain primary amphipathic cell-penetrating peptides (CPPs). These peptides have a primary structure that contains distinct hydrophobic and hydrophilic regions. Transportan (a chimeric peptide composed of galanin interlinked with mastoparan by a lysine) and MAP (an amphipathic model peptide) are two well-known CPPs that are considered to be members of the above mentioned class [11–14]. CPPs, also known as protein transduction domains (PTDs), in general have been used as transmembrane delivery vectors of hydrophilic molecules. Different mechanisms have been debated, but endocytosis followed by endosomal escape seems to dominate. There have been few sequence similarities found between different classes of CPPs, but nevertheless attempts to predict CPPs based on bulk properties of the constituent amino acids have been conducted with fair success [15]. The most common definitions of CPPs include a length restriction around 30 amino acids, a net positive charge and often either primary or secondary amphipathicity.

It has been shown that both the bovine and the mouse prion protein-derived peptides (abbreviated bPrPp(1–30), and mPrPp (1–28) respectively) can translocate over cell membranes even when coupled to large hydrophilic cargoes. Concomitantly these peptides cause cell toxicity and are thus not good candidates as useful CPPs [9,16]. However, the capability of crossing biomembranes suggests a plausible explanation for how oral prion infection might occur *in vivo*; an unprocessed PrP could in theory cross physiological barriers – like the gut epithelium or the blood brain barrier (BBB) – via a process where the CPP-like part of the protein would drag the rest of the prion protein (or an aggregated form of it) along as cargo. This type of *in vivo* protein transduction through the BBB has been demonstrated earlier for the Tat-β-galactocidase fusion protein (120 kDa) [17]. The Tat-peptide is a CPP derived from the protein transduction domain of the human immunodeficiency virus 1 (HIV-1) Tat protein [18].

This study focuses on the relevance of the NLS-like part of the PrP, *i.e.* residues 23–28 forming the KKRPKP-sequence. A new peptide, denoted mPrPp(23–50) (see Table 1 for peptide sequences), with the same length as mPrPp(1–28) and containing the KKRPKP-sequence was constructed. Its properties are compared to mPrPp(1–28) regarding membrane perturbation and translocation ability, both in membrane mimetic and living cell systems. The KKRPKP-sequence has been suggested to guide the cellular trafficking of PrP and to be responsible for direct internalization of the prion protein via endocytosis [19]. A recent study also shows that the PrP(23–30) sequence can selectively bind to PrP^{Sc} and not to PrP^C [20].

The present results that show great differences between the high and low membrane perturbing activites of mPrPp(1–28) and mPrPp(23–50), respectively, indicate that the KKRPKP segment may be necessary, but is not sufficient for the membrane perturbing activites of the unstructured part of PrP.

2. Materials and methods

2.1. Materials

1-palmitoyl-2-oleoyl-*sn*-glycero-3-phosphocholine (POPC) and 1-palmitoyl-2-oleoyl-*sn*-glycero-3-[phospho-*rac*-(1-glycerol)] sodium salt (POPG) were purchased from Avanti Polar Lipids, Alabaster, of best quality and used without further purification. Triton X-100 was obtained from Sigma. The prepacked PD-10 Columns, Sephadex™ G-25 M, were obtained from Amersham Biosciences. Calcein, a fluorescein derivative, was purchased from Molecular Probes, The Netherlands (product no. C-481). 5(6)-carboxyfluorescein and rhodamine-B-labelled dextran (70 kDa) were obtained from the same company.

The peptides (without fluorescent labels) were either purchased from Neosystem Laboratorie (Strasbourg, France) and used without further purification, or synthesized on a peptide synthesizer from Applied Biosystems (model 431A, USA). The *tert*-Butyloxycarbonyl amino acids and the *para*-methylbenzylhydrylamine (MBHA) resin were also acquired from Neosystem Laboratorie. Table 1 shows the sequences, relative hydrophobicities and Gibbs free energies of the studied peptides.

HeLa cells were obtained from the American Type Culture Collection (Manassas, USA). The cells were cultivated in Dulbecco's modified essential medium (DMEM) supplemented with 10% fetal bovine serum, 2 mM L-glutamine, 100 U ml^{-1} penicillin and 100 μg ml^{-1} streptomycin. All cell culture reagents were purchased from Invitrogen (Stockholm, Sweden).

2.2. Peptide synthesis, purification and analysis

2.2.1. Peptide synthesis and carboxyfluorescein labelling

The amino acids were linked in a stepwise manner in a 0.1 mmol scale on a peptide synthesizer using t-Boc strategy of solid phase peptide synthesis. *tert*-Butyloxycarbonyl amino acids were coupled as hydroxybenzotriazole (HOBt) esters to a *p*-methylbenzylhydrylamine (MBHA) to obtain C-terminally amidated peptides. The peptides were fluorescein labelled by the use of 5 molar equivalents of 5(6)-carboxyfluorescein, 5 molar equivalents of DIC, 5 molar equivalents of HOBt and 20 molar equivalents of DIEA in DMF (dimethylformamide) overnight. Deprotection of the formyl protecting group on tryptophan was carried out in 20% piperidine in DMF during 60 min. The peptides

Table 1
The peptide sequences examined in this study are given together with their average hydrophobicities calculated according to values devised by Kyte and Doolittle [33]

Peptide	Sequence	Net charge	Hydrophobicity
Melittin	GIGAVLKVLTTGLPALIS**W**IKRKRQQ	+5	0.27
mPrPp(1–28)	MANLG**Y**W**W**LLAL**F**VTM**W**TDVGLCKKRPKP	+3	0.30
Penetratin	RQIKI**WF**QNRRMK**W**KK	+7	−1.73
mPrPp(23–50)	KKRPKPGG**W**NTGGSR**Y**PGQGSPGGNRTP	+6	−1.86

Aromatic residues are written in bold, while charged residues are underlined.

were finally cleaved from the solid phase with HF (hydrogen fluoride) at 0 °C during 1 h in the presence of *p*-cresol, or *p*-cresol and *p*-thiocresol (1:1) if the peptide sequence contained cysteine or methionine residues.

2.2.2. HPLC purification and analysis of synthesized peptides

The cleaved peptides were purified using a reversed-phase HPLC Iomega C_{18} column and analyzed using a Perkin Elmer prOTOF™ 2000 MALDI O-TOF mass spectrometer.

2.2.3. Determination of peptide concentration

Peptides were dissolved in distilled water and the concentration of the solutions was established using a quartz cuvette of 1 cm path length in a CARY 4 spectrophotometer at 280 nm. The molar extinction coefficients used were 5690 M^{-1} cm^{-1} for tryptophan, 1280 M^{-1} cm^{-1} for tyrosine, and 120 M^{-1} cm^{-1} for cysteine [21].

2.3. Large unilamellar vesicles

2.3.1. Preparation of LUVs

Large unilamellar vesicles (LUVs) were prepared by dissolving the phospholipids POPC and POPG (in a desired molar ratio) in chloroform. The solution was vortexed in order to ensure proper mixing of the components, and the chloroform was evaporated using argon gas. The remaining lipid film was then placed under vacuum for a minimum time of 1 h in order to ensure the complete removal of residual chloroform. The dried lipid film was dispersed in 50 mM potassium phosphate buffer, pH 7.4, by vortexing (10 min) resulting in a final lipid concentration of either 1 or 10 mM (based on weight to volume). The dispersion was freeze–thawed five times using liquid nitrogen/hot water and then passed through two membranes of 100 nm pore size 21 times using a pneumatic Avanti extruder. The vesicles were kept on ice when not involved in measurements and always used within 24 h.

2.3.2. Preparation of calcein-entrapping LUVs

A 55 mM calcein solution in 50 mM potassium phosphate buffer pH 7.4 was prepared. The solution was passed once through two 100 nm pore sized membranes before it was used to disperse a dried lipid film of desired composition. The resulting 10 mM lipid dispersion was vortexed, freeze–thawed and extruded as described above. The formed calcein-entrapping vesicles were passed through three sequential Sephadex-G25 columns in order to remove the non-entrapped calcein. The dilution factor of each column is estimated to be ~1.5 according to the manufacturer.

2.4. Steady-state fluorescence spectroscopy

The calcein leakage measurements were conducted on a Perkin Elmer LS 50B Luminescence Spectrometer using FL WinLab software. The experiments were run at room temperature in a 4×10 mm quartz cuvette. The samples were excited at 490 nm and their emission was scanned from 510 to 600 nm. The scan speed was 250 nm/min and the bandwidth for both excitation and emission was set to 4 nm. Each spectrum was baseline corrected and averaged over five accumulated scans. The fluorescence of calcein is well self-quenched at 55 mM.

2.4.1. Peptide-induced calcein leakage from calcein-entrapping LUVs

Calcein-entrapping LUVs POPC:POPG (4:1) were diluted with 50 mM potassium phosphate buffer pH 7.4 to a phospholipid concentration of ~400 μM and 750 μl was used for each experiment. Each peptide (stock solution 100 μM) was titrated into the sample (3 μl at a time) with an incubation time of 3 min preceding each measurement. The vesicles were lysed with 5 μl of 10% (v/v) Triton X-100 at the end of each titration series in order to establish the maximum fluorescence intensity corresponding to each sample. The % leakage was determined according to:

$$\%\,\text{leakage} = 100\left(\frac{F - F_0}{F_{\max} - F_0}\right)$$

where F_0 represents the background fluorescence, $F_{\max}$ the fluorescence after lysis of the vesicles, and F the fluorescence upon 3 min incubation of the vesicles with the peptide.

2.5. Spectrophotometry

For the measurement of haemoglobin leakage, a CARY 4 Spectrophotometer was used combined with a quartz cuvette with a 1 cm light path. The absorption was measured at the haemoglobin absorption maximum of 540 nm and averaged over three measurements.

2.5.1. Peptide-induced haemoglobin leakage from hRBCs

Peptides were tested for haemolytic activity against human red blood cells (hRBCs) taken from fresh venous blood. The hRBCs were washed three times with buffer (150 mM NaCl, 0.1 mM EDTA, 20 mM Tris, pH 7.4) by centrifugation (10 min, 3000 rpm, 10 °C) and re-suspension. The rinsed blood cells were then diluted with buffer to a concentration of about 5% v/v hRBCs, (haematocrit) and distributed to 15 ml falcon tubes (1 ml of diluted blood in each). Peptides (10 μM) were added to the falcon tubes and incubated for different time periods during rocking at room temperature. The blood was then centrifuged again (2 min, 3000 rpm, 10 °C) and the supernatant was analyzed by spectrophotometry as described above. 0% and 100% haemolytic activity was defined by the absorption of the supernatant of hRBCs suspended in buffer and water respectively. The apparent percentage haemolysis was calculated according to:

$$\%\,\text{haemolysis} = 100\left(\frac{A_t - A_0}{A_{\max} - A_0}\right)$$

where A_0 is the background absorption level, $A_{\max}$ the level after cell lysis, and A_t the measured absorption at time t after addition of the peptide.

2.6. Circular dichroism spectroscopy (CD)

CD measurements were conducted on a Jasco-750 CD Spectropolarimeter with a 1 mm quartz cuvette. The spectra were acquired from 260 to 190 nm with a data pitch of 1 nm. The scanning speed was 50 nm/min, the response time 1 s and the slit width 2 nm. Each spectrum was background corrected and averaged over 15 accumulated scans. The mean residual molar ellipticities were calculated with respect to peptide concentration, light path length and number of residues. The LUVs (POPC:POPG (4:1) or POPC) where diluted with 50 mM phosphate buffer, pH 7.4, to a total lipid concentration of 100 μM. Peptides (total concentration 20 μM) were incubated at room temperature for 30 min with the LUVs before measurements. Reference spectra were run in water and buffer. All experiments were conducted at 25 °C.

2.7. Peptide translocation and toxicity studies on HeLa cells

2.7.1. Co-localization of mPrPp(1–28) and mPrPp(23–50) with dextran in live HeLa cells

HeLa cells were seeded in NUNC 8-well chambers and one day post seeding, at an 80% confluence, the cells were washed with serum-free DMEM, followed by the addition of the peptides at a final concentration of 2 μM. After 30 min incubation, the cells were washed three times with HKR (Hepes buffered Krebs–Ringer) buffer (containing 125 mM NaCl, 3.5 mM KCl, 1.5 mM $CaCl_2$, 1.2 mM $MgSO_4$, 1.25 mM KH_2PO_4, 25 mM $NaHCO_3$, 10 mM HEPES, and 10 mM D-glucose, pH 7.4). After washing, fluoresceinyl-labelled peptide and rhodamine-B-labelled dextran were added simultaneously at a final concentration of 2 μM and 1 mg ml^{-1}, respectively. After 30 min incubation in serum-free DMEM at 37 °C, the cells were washed three times with HKR buffer and examined using UltraView ERS confocal live cell imager (PerkinElmer Ltd, Upplands-Väsby, Sweden) connected to an Axiovert 200 (Zeiss, Göttingen, Germany). Negative controls were made without the presence of dextran.

2.7.2. Cytotoxicity of prion protein-derived peptides measured by LDH leakage

HeLa cells were seeded out in 48-well plates 2 days before the experiments, and at 80% confluency the membrane integrity was assessed using the Promega Cytox-ONE™ assay. Cytotoxicity was expressed as the percent extracellular lactase dehydrogenase (LDH) activity out of the total LDH activity measured after cell lysis. HeLa cells were incubated with different

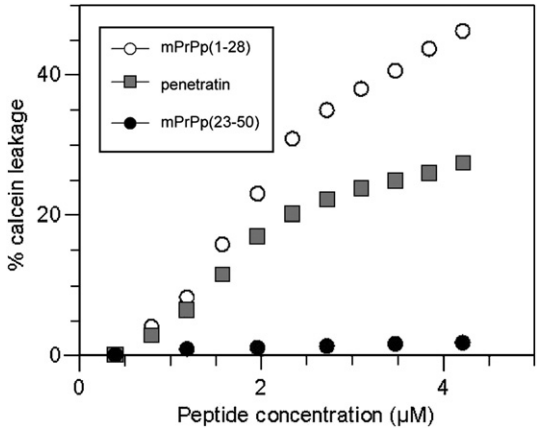

Fig. 1. The induced calcein leakage in 400 μM POPC:POPG (4:1) LUVs, pH 7.4. 3 μl of 100 μM peptide was added and incubated for 3 min before each measurement. All experiments were conducted at room temperature.

concentrations of peptide at 37 °C during 30 min. The cytotoxic effects of the PrP-derived peptides were compared to the ones of penetratin and melittin. The experiments were repeated three times on independent duplicate cells.

3. Results

Previous studies [22] concerning mPrPp(1–28), penetratin and melittin in partially charged large unilamellar vesicles (LUVs) showed significant differences in their abilities to cause leakage of vesicle entrapped calcein. Melittin is the main constituent of the toxin from honeybee, *Apis mellifera*, and known to be a very potent membrane perturbing peptide [23]. Penetratin is a relatively non-toxic, but efficient CPP [24]. Melittin was found to cause rapid and complete calcein leakage in the LUVs, followed by mPrPp(1–28) with intermediate activity, and penetratin being relatively inert [22]. In the present study we investigated the effects of mPrPp(23–50) in a similar, partially negatively charged membrane model system comparing the results to mPrPp(1–28) and penetratin. The peptide-induced release of calcein from the calcein-entrapping LUVs is shown in Fig. 1 as a function of peptide concentration. In these

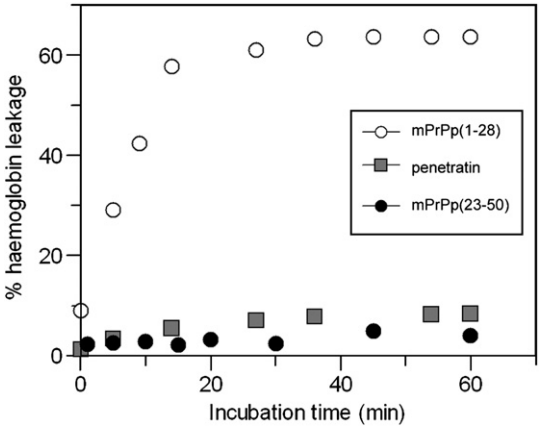

Fig. 2. The percentual haemoglobin leakage from hRBC after incubation with 10 μM peptides during different time periods. Experiments were conducted at room temperature at pH 7.4.

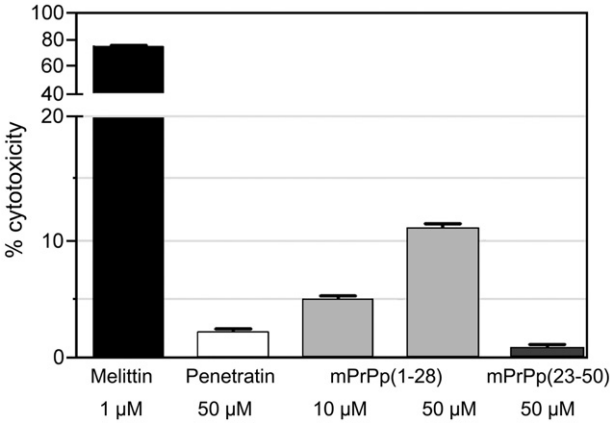

Fig. 3. The percentual cytotoxicity of four different peptides based on lactate dehydrogenase (LDH)-leakage in HeLa cells. The incubation time was 30 min at 37 °C for all measurements. The enzyme activity after peptide treatment was expressed as the percentage of extracellular LDH activity as compared to the total LDH activity measured upon cell lysis. The standard error of mean was calculated based on three independent duplicates of experiments.

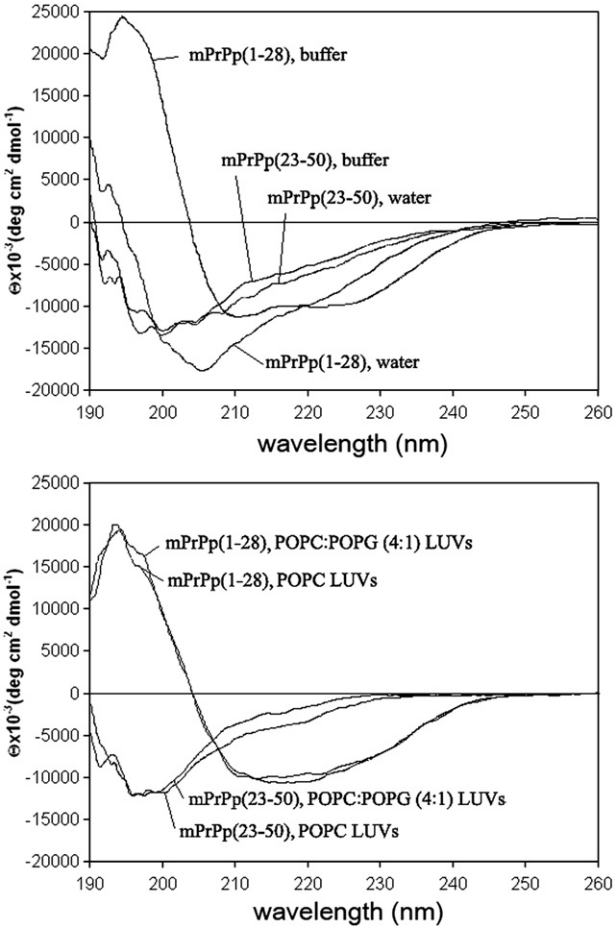

Fig. 4. (Top) The CD spectra of mPrPp(1–28) and mPrPp(23–50) in water and 50 mM potassium phosphate buffer, pH 7.4. (Bottom) The CD spectra of mPrPp (1–28) and mPrPp(23–50) with LUVs in the same buffer with either POPC or POPC:POPG (4:1) content, and a total lipid concentration of 100 μM. All measurements were conducted at 25 °C after 30 min of incubation with 20 μM peptide at room temperature.

experiments increasing amounts of peptide were titrated onto the vesicle sample, which was incubated for 3 min before each measurement. As expected, the results show that mPrPp(1–28) is more potent than penetratin in leakage induction potency. In contrast to the two peptides which were able to induce vesicle leakage, mPrPp(23–50) did not give rise to any significant leakage from the LUVs.

In another experiment, the haemolytic activities of the three peptides were investigated. Here, the peptide-induced haemoglobin leakage in human erythrocytes was followed at 10 μM peptide concentrations. Fig. 2 shows the time course of haemoglobin leakage for mPrPp(1–28), mPrPp(23–50) and penetratin. Under these conditions there is significant haemoglobin leakage caused only by mPrPp(1–28). mPrPp(23–50) is even somewhat less haemolytic than penetratin.

Next we investigated a more complex cell system for the sensitivity towards the peptides. Lactate dehydrogenase (LDH) leakage from HeLa cells was used as a measure of the cytotoxic effects of the two PrP-derived peptides. In this case we chose to compare the effects to both penetratin and melittin, the latter used to give a high degree of leakage close to what is observed after cell lysis. The LDH activity was measured outside the HeLa cells after an incubation time of 30 min and compared to the total LDH activity measured upon cell lysis, defining 100% cytotoxicity. Fig. 3 shows that melittin reaches a level of almost 80% cytotoxicity already at a concentration of 1 μM, whereas penetratin and mPrPp(23–50) stay at levels of 1–3% at a concentration of 50 μM. The more active mPrPp(1–28) on the other hand, reaches levels that could be considered cytotoxic (*i.e.* above 10%) at 50 μM concentration, while at 10 μM the cytotoxicity can still be considered low—around 5%.

Fig. 4 displays the CD spectra of the two mPrP-derived peptides, 20 μM, in water, 50 mM sodium phosphate buffer pH 7.4, and in the presence of POPC:POPG (4:1) and POPC LUVs at pH 7.4. No significant change from random coil is induced by neither buffer nor the presence of vesicles in the case of mPrPp(23–50) after an incubation time of 30 min. This result suggests overall very weak (and/or slowly occurring) interactions (if any) with the vesicular membranes, even with the charged LUVs. mPrPp(1–28) on the other hand, changes its secondary structure depending on its environment. In water, it predominantly takes on a random coil structre, while buffer seems to stabilize an α-helical conformation. In both zwitterionic and negatively charged LUVs we observe a conversion towards a mixture of β-sheet and α-helix for mPrPp(1–28). At 50 μM concentration both peptides have however shown a propensity towards aggreggation after prolonged room temperature exposure in buffer containing samples (data not shown).

In order to establish whether the two mPrP-derived peptides show different translocation abilities upon contact with biological membranes, confocal fluorescence microscopy was used to study their internalization potency in live HeLa cells. For these experiments, fluoresceinyl-labelled peptides had to be used. Fig. 5 shows the confocal microscopy images of live HeLa cells together with mPrPp(1–28) in the left column, and mPrPp (23–50) in the right column. The cells still look intact after 30 min of incubation with both peptides. Distinct fluorescent spots are visible for mPrPp(1–28), showing membrane translocation into the cells for this peptide, in agreement with previous studies [9,16]. Under the same conditions for mPrPp(23–50), the absence of fluorescent spots inside the cells shows that mPrPp (23–50) has a much weaker ability to enter into the cells.

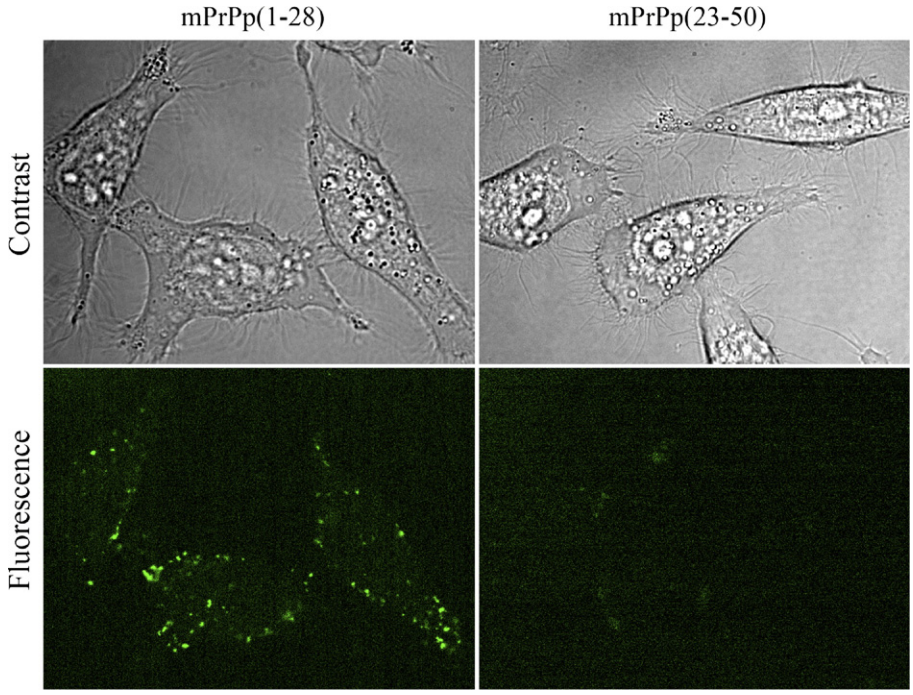

Fig. 5. Confocal microscopy images of live HeLa cells showing the internalized fluoresceinyl-labelled mPrPp(1–28) and mPrPp(23–50). mPrPp(1–28) is effectively internalized, whereas mPrPp(23–50) is just barely internalized. The incubation time was 30 min at 37 °C and the final peptide concentration 2 μM.

Although such images are difficult to interpret quantitatively, we suggest that the experiment shows a significant difference between the two peptides in their cell-penetrating ability, with mPrPp(1–28) being significantly more potent. Further confocal microscopy experiments with the labelled peptides confirmed the quantitative difference in their uptake into live HeLa cells (Fig. S1). These images also showed that mPrPp(1–.28) co-localizes with dextran, a fluid-phase endocytosis marker, suggesting fluid-phase endocytosis to be a dominant mechanism of internalization for this peptide. In some experiments very small traces of mPrPp(23–50) could be observed inside the HeLa cells (data not shown), which may suggest that this peptide is internalized by random incorporation of outside materials during endocytosis.

4. Discussion

In this study we investigate the significance of the basic KKRPKP-sequence, residues 23–28 of the mouse prion protein, by constructing a peptide mPrPp(23–50), with this basic sequence overlapping with mPrPp(1–28). Three types of experiments to investigate membrane perturbation caused by mPrPp(23–50) comparing it to mPrPp(1–28) were performed. Calcein leakage from partially charged LUVs, leakage of haemoglobin from erythrocytes as well as LDH leakage from HeLa cells showed very similar patterns: compared to the rather potent mPrPp(1–28) which had been studied earlier [22], mPrPp(23–50) was found to be inactive. The parallel membrane perturbations effects in model systems as well as in cell systems suggest that despite the obvious differences in membrane composition in the experiments, there is a fundamental phospholipid bilayer interaction which may be the major factor to determine the extent of cell leakage and toxicity. The behaviour of the prion derived peptides in this experiment approximately follows the calculated hydrophobicity index of respective peptides, as indicated by Table 1. The positive hydrophobicities of melittin and mPrPp(1–28) are compatible with their high membrane perturbing activities, whereas the negative hydrophobicities of penetratin and mPrPp(23–50) are compatible with their low membrane perturbing activities, although there is no absolute relationship between the theoretical indices and the experimental observations.

The importance of direct membrane perturbation during an induced cell response, is suggested also from comparing the membrane perturbation results (Figs. 1–3) to the secondary structures obtained by CD (Fig. 4). mPrPp(1–28) interactions with vesicle membranes, uncharged or partially charged, are seen as changes in secondary structure. The peptide intreracts with both types of membranes in the same conformation, suggesting that the mode of action is similar as well. mPrPp (23–50) does not show any obvious interaction with the vesicles judging from the lack of structure induction observed by CD. In itself an unchanged CD spectrum is not a proof of absence of membrane interaction, since for example the dynorphin opioid peptides [25,26] are known to translocate through cell membranes and still retain their random coil formations. We conclude however, that the weak membrane perturbations exhibited by mPrPp(23–50) in general, are in line with the absence of secondary structure induction by the vesicle membranes.

Fig. 5 compares the ability of fluorecein-labelled mPrPp (1–28) and mPrPp(23–50) to enter into live HeLa cells. Again mPrPp(23–50) is much less active than mPrPp(1–28). The mPrPp(1–28) peptide is highly homologous to its bovine counterpart bPrPp(1–30), which has previously been shown to enter live mammalian CHO cells [16] using macropinocytosis (fluid-phase endocytosis) as the main mechanism of action. The same conclusion is drawn here for mPrPp(1–28) based on co-localization experiment with dextran shown in Fig. S1. The significantly different membrane perturbation activites of the mPrPp(1–28) and mPrPp(23–50) correlate well with their respective cell membrane translocation abilities.

The signal sequence of the prion protein, residues 1–22 in mPrP, is normally cleaved off during maturation, but it has been shown that this process might fail at times leaving the signal sequence in place [6]. The retention of the signal sequence has been suggested to prompt the prion protein's conformational change from the cellular, benign form, to the neurotoxic scrapie form [6,9]. In the native protein, the signal sequence is followed by a basic region (KKRPKP) referred to as the NLS-like sequence. The results presented in this study show that in a peptide or unstructured part of a protein the KKRPKP-sequence in itself is not sufficient to cause potent membrane perturbations or to mediate cell transloction. We propose that the KKRPKP-sequence needs a hydrophobic partner sequence in order to attain membrane perturbation and translocation properties. One can question whether the hydrophobic segment has to be adjacent like the signal peptide (residues 1–22) in the present case, or whether the membrane activity can be efficiently increased by a hydrophobic segment present elsewhere in the protein sequence. Possibly the putative transmembrane region around residue 115 (still a part of the unstructured N-terminus) could fulfil this role in PrP. The hydrophobicity of mPrPp(1–28) is higher than that of mPrPp(23–50) (Table 1) which is in line with the observation that mPrPp(23–50) has more difficulty to dissolve itself into the bilayer. Although the net positive charge is higher for mPrPp(23–50) (which would facilitate initial contact with the negatively charged membranes via electrostatic interactions) this is obviously not the major determining factor for the membrane activities investigated in the present study.

The mPrPp(1–28) has the theoretical ability to form an amphipathic helix based on helical wheel projections and may therefore, in parallel to the endocytotic mechanism, internalize by transient pore formation or disruption of the bilayer according to the carpeting model. These latter mechanisms are related to what has been described earlier for anti-microbial peptides among others [27,28]. Since the CD-data clearly shows a mixture of induced α-helix and β-sheet for mPrPp(1–28) when interacting with the LUVs, we cannot rule out these as complementary mechanisms. The presence of an unprocessed signal peptide in the PrP may cause not only toxicity through

transient pore formation, but also mediate aggregation that might lead to the structure conversion of PrP^{C} to PrP^{Sc}. In addition, the CPP-like activity of the N-terminus of the unprocessed protein, could be important in the transmission process of TSE diseases. Binding to negatively charged cell surface heparan sulphates, would provide the main route of entry to the cell by endocytosis [16]. How PrP conversion takes place is still unknown, but several studies suggest that lipid rafts might play a key role in the process [29] and cholesterol depletion has been shown to decrease conversion of PrP^{C} to PrP^{Sc} [30]. An infection propagation by direct cell membrane contacts has also been proposed [31]. It is worth noting that among the common "amyloid" related proteins, only PrP has a hydrophobic signal sequence directly followed by a basic sequence [32]—the combination of which should be responsible for the CPP-like property of this domain.

In conclusion, the NLS-like (23–28) sequence KKRPKP in the prion protein requires addition of a hydrophobic segment like an uncleaved signal peptide (1–22) sequence to bring about potent membrane perturbing activities. The addition of the more hydrophilic (29–50) peptide sequence does not mediate this activity. The results indicate that a prion protein with an uncleaved signal sequence in its unstructured N-terminus should be much more perturbing to cellular membranes than its properly processed form without signal peptide.

Acknowledgements

We thank Dr Jens Danielsson for valuable help with the hBRCs sampling. We also thank Mr Torbjörn Astlind for expert instrumental assistance. The study was supported by grants from the Swedish Research Council, subject areas: Natural Science and Technology; Medicine (VR-NT and VR-M), and the European Commission, contract LSHG-CT-2004-512051.

Appendix A. Supplementary data

Supplementary data associated with this article can be found, in the online version, at doi:10.1016/j.bbamem.2007.09.034.

References

[1] S.J. Collins, V.A. Lawson, C.L. Masters, Transmissible spongiform encephalopathies, Lancet 363 (2004) 51–61.
[2] S.B. Prusiner, Molecular biology of prion diseases, Science 252 (1991) 1515–1522.
[3] B. Caughey, P.T. Lansbury, Protofibrils, pores, fibrils, and neurodegeneration: separating the responsible protein aggregates from the innocent bystanders, Annu. Rev. Neurosci. 26 (2003) 267–298.
[4] D.A. Kocisko, J.H. Come, S.A. Priola, B. Chesebro, G.J. Raymond, P.T. Lansbury, B. Caughey, Cell-free formation of protease-resistant prion protein, Nature 370 (1994) 471–474.
[5] B. Drisaldi, J. Coomaraswamy, P. Mastrangelo, B. Strome, J. Yang, J.C. Watts, M.A. Chishti, M. Marvi, O. Windl, R. Ahrens, F. Major, M.S. Sy, H. Kretzschmar, P.E. Fraser, H.T. Mount, D. Westaway, Genetic mapping of activity determinants within cellular prion proteins: N-terminal modules in PrP^{C} offset pro-apoptotic activity of the Doppel helix B/B′ region, J. Biol. Chem. 279 (2004) 55443–55454.
[6] R.S. Stewart, B. Drisaldi, D.A. Harris, A transmembrane form of the prion protein contains an uncleaved signal peptide and is retained in the endoplasmic reticulum, Mol. Biol. Cell 12 (2001) 881–889.
[7] S.J. Kim, R. Rahbar, R.S. Hegde, Combinatorial control of prion protein biogenesis by the signal sequence and transmembrane domain, J. Biol. Chem. 276 (2001) 26132–26140.
[8] C.M. Ott, V.R. Lingappa, Signal sequences influence membrane integration of the prion protein, Biochemistry 43 (2004) 11973–11982.
[9] P. Lundberg, M. Magzoub, M. Lindberg, M. Hällbrink, J. Jarvet, L.E.G. Eriksson, Ü. Langel, A. Gräslund, Cell membrane translocation of the N-terminal (1–28) part of the prion protein, Biochem. Biophys. Res. Commun. 299 (2002) 85–90.
[10] T. Boulikas, Putative nuclear localization signals (NLS) in protein transcription factors, J. Cell Biochem. 55 (1994) 32–58.
[11] J. Oehlke, A. Scheller, B. Wiesner, E. Krause, M. Beyermann, E. Klauschenz, M. Melzig, M. Bienert, Cellular uptake of an alpha-helical amphipathic model peptide with the potential to deliver polar compounds into the cell interior non-endocytically, Biochim. Biophys. Acta 1414 (1998) 127–139.
[12] M. Pooga, Cell penetrating peptide, transportan, and its predecessors, galanin-based chimeric peptides, ed., Tartu (1998).
[13] A. Scheller, J. Oehlke, B. Wiesner, M. Dathe, E. Krause, M. Beyermann, M. Melzig, M. Bienert, Structural requirements for cellular uptake of alpha-helical amphipathic peptides, J. Pept. Sci. 5 (1999) 185–194.
[14] A. Scheller, B. Wiesner, M. Melzig, M. Bienert, J. Oehlke, Evidence for an amphipathicity independent cellular uptake of amphipathic cell-penetrating peptides, Eur. J. Biochem. 267 (2000) 6043–6050.
[15] T. Holm, S. Netzereab, M. Hansen, Ü. Langel, M. Hällbrink, Uptake of cell-penetrating peptides in yeasts, FEBS Lett. 579 (2005) 5217–5222.
[16] M. Magzoub, S. Sandgren, P. Lundberg, K. Oglęcka, J. Lilja, A. Wittrup, L.E.G. Eriksson, Ü. Langel, M. Belting, A. Gräslund, N-terminal peptides from unprocessed prion proteins enter cells by macropinocytosis, Biochem. Biophys. Res. Commun. 348 (2006) 379–385.
[17] S.R. Schwarze, A. Ho, A. Vocero-Akbani, S.F. Dowdy, In vivo protein transduction: delivery of a biologically active protein into the mouse, Science. 285 (1999) 1569–1572.
[18] E. Vivès, P. Brodin, B. Lebleu, A truncated HIV-1 Tat protein basic domain rapidly translocates through the plasma membrane and accumulates in the cell nucleus, J. Biol. Chem. 272 (1997) 16010–16017.
[19] C. Sunyach, A. Jen, J. Deng, K.T. Fitzgerald, Y. Frobert, J. Grassi, M.W. McCaffrey, R. Morris, The mechanism of internalization of glycosylphosphatidylinositol-anchored prion protein, Embo J. 22 (2003) 3591–3601.
[20] A.L. Lau, A.Y. Yam, M.M. Michelitsch, X. Wang, C. Gao, R.J. Goodson, R. Shimizu, G. Timoteo, J. Hall, A. Medina-Selby, D. Coit, C. McCoin, B. Phelps, P. Wu, C. Hu, D. Chien, D. Peretz, Characterization of prion protein (PrP)-derived peptides that discriminate full-length PrP^{Sc} from PrP^{C}, Proc. Natl. Acad. Sci. U. S. A. 104 (2007) 11551–11556.
[21] S.C. Gill, P.H. von Hippel, Calculation of protein extinction coefficients from amino acid sequence data, Anal. Biochem. 182 (1989) 319–326.
[22] M. Magzoub, K. Oglęcka, A. Pramanik, L.E.G. Eriksson, A. Gräslund, Membrane perturbation effects of peptides derived from the N-termini of unprocessed prion proteins, Biochim. Biophys. Acta 1716 (2005) 126–136.
[23] N. Koyama, K. Hirata, K. Hori, K. Dan, T. Yokota, Biphasic vasomotor reflex responses of the hand skin following intradermal injection of melittin into the forearm skin, Eur. J. Pain 6 (2002) 447–453.
[24] D. Derossi, G. Chassaing, A. Prochiantz, Trojan peptides: the penetratin system for intracellular delivery, Trends Cell Biol. 8 (1998) 84–87.
[25] J. Lind, A. Gräslund, L. Mäler, Membrane interactions of dynorphins, Biochemistry 45 (2006) 15931–15940.
[26] L. Hugonin, V. Vukojevic, G. Bakalkin, A. Gräslund, Membrane leakage induced by dynorphins, FEBS Lett. 580 (2006) 3201–3205.
[27] J. Fernandez-Carneado, M.J. Kogan, S. Pujals, E. Giralt, Amphipathic peptides and drug delivery, Biopolymers 76 (2004) 196–203.
[28] K. Takeshima, A. Chikushi, K.K. Lee, S. Yonehara, K. Matsuzaki, Translocation of analogues of the antimicrobial peptides magainin and buforin across human cell membranes, J. Biol. Chem. 278 (2003) 1310–1315.
[29] A. Taraboulos, M. Scott, A. Semenov, D. Avrahami, L. Laszlo, S.B.

Prusiner, Cholesterol depletion and modification of COOH-terminal targeting sequence of the prion protein inhibit formation of the scrapie isoform, J. Cell. Biol. 129 (1995) 121–132.
[30] G.S. Baron, K. Wehrly, D.W. Dorward, B. Chesebro, B. Caughey, Conversion of raft associated prion protein to the protease-resistant state requires insertion of PrP-res (PrP(Sc)) into contiguous membranes, Embo J. 21 (2002) 1031–1040.
[31] K. Simons, R. Ehehalt, Cholesterol, lipid rafts, and disease, J. Clin. Invest. 110 (2002) 597–603.
[32] M. Stefani, C.M. Dobson, Protein aggregation and aggregate toxicity: new insights into protein folding, misfolding diseases and biological evolution, J. Mol. Med. 81 (2003) 678–699.
[33] J. Kyte, R.F. Doolittle, A simple method for displaying the hydropathic character of a protein, J. Mol. Biol. 157 (1982) 105–132.